Q. J. R. Meteorol. Soc. (2003), **129**, pp. 1761–1778 doi: 10.1256/qj.02.83

Layer-wise attribution of vertical motion and the influence of potential-vorticity anomalies on synoptic development

By M. A. G. DIXON*, A. J. THORPE and K. A. BROWNING
Joint Centre for Mesoscale Meteorology, University of Reading, UK

(Received 3 March 2002; revised 22 October 2002)

SUMMARY

A methodology is presented for attributing vertical motion to potential vorticity (PV) in a explicit manner using the quasi-geostrophic omega equation. The methodology is then used to determine the contribution individual PV anomalies make to the synoptic development. It is shown how the total vertical motion may be decomposed into self-generating and interaction terms. The former correspond to vertical motion that arises from one PV region alone, whilst each of the interaction terms represent vertical motion due to the interaction of two different regions of PV. The method is applied to a number of cyclones studied in the Fronts and Atlantic Storm-Tracks Experiment in order to determine the dynamical role of individual PV regions in cyclogenesis. For purposes of comparison, cyclones were chosen to be representative of the types (A, B and C) of an extended Petterssen–Smebye scheme devised by Deveson, Browning and Hewson. In terms of our new PV method, the Type A and B cyclones exhibit only subtle differences, with the upper-level layer of PV playing a larger role in the case of the Type B cyclone. A much larger difference is apparent between the Type A and B cyclones on the one hand, and the Type C cyclone on the other: in the Type C cyclone, the upper-level PV self-generating term plays an important role, whereas in the Type A and B cases the influence of the upper-level PV is largely restricted to the interaction terms. In all of the cases, the vertical motion attributable to the interaction between the low-level PV and boundary thermal gradient was found to be large. Hence, from the viewpoint of instantaneous attribution, we conclude that the low-level PV is always important.

KEYWORDS: Cyclone classification Cyclogenesis FASTEX

1. INTRODUCTION

This paper sets out a methodology by which vertical motion may be attributed to regions of quasi-geostrophic (QG) potential vorticity (PV) in an explicit manner. It is shown that, for a given decomposition of the total QGPV distribution, there exists a corresponding decomposition of the vertical motion, wherein each of its components is *uniquely* attributable to either one or two regions of PV. The methodology establishes a diagnostic link between PV and dynamical development. We demonstrate the usefulness of this link by considering the specific case of midlatitude cyclone development.

It has been recognized that PV-thinking provides a powerful way of understanding dynamical development (Hoskins *et al.* 1985, hereafter referred to as HMR). Apart from the inherent interest of determining the dynamical significance of a particular region of PV, there are at least two advantages of doing so from the viewpoint of forecasting. As PV (in the absence of irreversible processes) is materially conserved, it is relatively easy to predict the advection of a given PV region. Thus, if at a given instant one could determine which PV region is most dynamically significant, observations could be targeted so that the PV region is accurately assimilated into an analysis at a later time. By way of contrast, if one were to view vertical motion in terms of sources that are not materially conserved, then the procedure of targeting would become more difficult.

Determining which regions of PV are dynamically significant may also be helpful in terms of model improvement. PV provides a link between irreversible processes and their ensuing effects on the dynamics. That is, irreversible processes lead to local changes in the PV distribution which, in turn, may lead to dynamical development. Given this property, it is an attractive idea to validate model parametrizations of irreversible processes in terms of the PV anomalies created.

* Corresponding author: Joint Centre for Mesoscale Meteorology (JCMM), Meteorology Building, University of Reading, PO Box 243, Earley Gate, Reading Berkshire RG6 6BB, UK. e-mail: mark.dixon@metoffi ce.com

The attribution of vertical motion *per se* is a well-known technique of analysing dynamical development. The procedure normally adopted involves the use of an omega equation, wherein the total vertical motion is partitioned into components attributable to particular 'sources'. A number of sources have been considered, including the 'traditional' choices of thermal advection (TA) and differential vorticity advection (VA). This choice of source underpins the cyclone classification scheme of Petterssen and Smebye (1971) (hereafter referred to as PS). The frame-independent choice of $\nabla \cdot \mathbf{Q}$ (Hoskins *et al.* 1978; Clough *et al.* 1996) has recently been used by Deveson *et al.* (2002) (hereafter referred to as DBH) to develop a modified version of the PS scheme. According to this scheme, cyclones are classified partly in terms of the relative importance of the upper- and lower-level distributions of $\nabla \cdot \mathbf{Q}$. It is important to note, however, that neither of these schemes directly addresses the question of cyclone development in terms of PV.

Two versions of so-called 'PV-surgery' have been adopted in an attempt to attribute dynamic effects to specific regions of PV. On the one hand, some studies (e.g. Davis 1992; Davis and Emanuel 1991; Griffiths *et al.* 2000; Morgan 1999; Stoelinga 1996; Thorpe 1997) assess the dynamical significance of a PV region in a *diagnostic* sense either by calculating the difference in vertical motion between an unaltered atmospheric state and another where the PV region has been removed, or by assessing the effect on development of the horizontal-wind fields attributable to a region of PV. The alternative *prognostic* approach involves measuring the impact on a time-evolving model of removing the PV region from the initial model state (Ahmadi-Givi and Craig (personal communication); Swarbrick 2001). Both approaches share a common feature: the dynamical impact, which is nominally attributed to a particular PV region, depends upon the rest of the total PV distribution.

The diagnostic methodology presented in this paper partitions the total QG vertical motion, which is nominally attributable to a given region of PV, into several components. Each component is attributable either to that PV region alone (the so-called 'self-generating' part), or to the 'interaction' between the region and other 'elements' in the domain, where these elements are either PV regions or are identified with boundary conditions. Whilst the resulting conceptual picture is complicated by the existence of the 'interaction' terms, it is argued that this is, nevertheless, an appropriate way in which to proceed with the diagnostic PV attribution of vertical motion. The usefulness of the methodology in determining the dynamical significance of PV regions is illustrated via case studies of midlatitude cyclones. For simplicity, we have adopted a 'layer-wise' approach, wherein the total PV distribution is partitioned into three components, viz. an upper and a lower slab, and an infinitesimal layer at the surface. Such a partitioning also facilitates a comparison with the DBH classification scheme. We wish to determine the difference between attributing dynamical development to PV on the one hand, and to regions of $\nabla \cdot \mathbf{Q}$ on the other hand. Thus, we apply our methodology to cyclones representative of the three classes (Types A, B and C) of the DBH scheme. The methodology does not explicitly take into account the effects of irreversible processes. However, to a certain extent, irreversible forcing can be viewed as being 'slaved' to the purely dynamical forcing. Hence, we assume that the results will be indicative of the importance of PV notwithstanding the presence of irreversible processes.

2. The omega equation

The QG omega equation can be written as:

$$\mathrm{L}(\omega) = S, \tag{1}$$

where the operator

$$\mathrm{L} \equiv \nabla_p^2 + \frac{f_0^2}{\sigma}\frac{\partial^2}{\partial p^2}, \tag{2}$$

and $\omega = \mathrm{D}p/\mathrm{D}t$, p is the pressure, f_0 is the Coriolis parameter, σ is the horizontally averaged static stability, and the subscript p denotes that the 2-D Laplacian is applied on a constant pressure surface.

Clough *et al.* (1996) used an electrostatics analogy as an illuminating way of physically interpreting Eq. (1), wherein the source term, S, is analogous to a distribution of charge and ω, which in this paper is referred to as the *vertical motion*, is akin to the electric potential associated with that charge. Thus, the vertical-motion field is said to be *attributable* to the source distribution. In a similar manner, the stream function can be attributed to the PV distribution (see Bishop and Thorpe (1994) and section 3 below). This paper is concerned with 'layer-wise' attribution, i.e. the process by which the total ω is partitioned into components, each of which is attributable to a layer of S. We next consider the various mathematical formulations of S which were referred to in the introductory section. The physical interpretation of each, along with some of the ways in which the resulting conceptual pictures have been applied in the literature, is discussed.

(*a*) *Traditional formulation*

The traditional form of the source term (see, for example, Hoskins *et al.* (1978)) is given by:

$$S = f_0\frac{\partial}{\partial p}\{(\mathbf{v}-\mathbf{c})\cdot\nabla_p\xi\} + R\nabla^2\{(\mathbf{v}-\mathbf{c})\cdot\nabla_p\theta\}, \tag{3}$$

where $\mathbf{c}$ is the velocity of the reference frame with respect to which the velocity fields $\mathbf{v}$ are expressed, ξ is the vorticity, θ is the potential temperature, and R is the universal gas constant. The two terms are referred to as (differential) vorticity advection (VA) and thermal advection (TA), respectively.

Petterssen and Smebye (1971) set out a classification scheme (PS) which defines two types of cyclone. Generally speaking*, 'Type A' cyclones are those that are predominately forced by TA in the lower part of the atmosphere, whereas 'Type B' cyclones are forced mainly by VA in the upper levels. However, from (3) it is clear that both VA and TA are dependent on the choice of $\mathbf{c}$. Hence, such a classification scheme is ambiguous since the determination of whether TA or VA dominates in a particular cyclone requires a reference frame to be specified. Such ambiguity has long been appreciated, and the 'Q-vector' formulation of the omega equation introduced by Hoskins *et al.* (1978) is a method of avoiding such difficulties.

(*b*) *Q-vector formulation*

In this formulation the source is given by:

$$S = -2\nabla\cdot\mathbf{Q}. \tag{4}$$

* The PS scheme does in fact use further criteria to distinguish the two types of cyclone, such as the relative distance between upper-level troughs and surface lows; more to the point, it makes reference the time-dependency of such quantities. Nevertheless, the distinction described in the text here is the main determinant of whether a cyclone is of type A or B.

The longitudinal (λ) and latitudinal (ϕ) components of the Q-vector, $\mathbf{Q} = [Q_1, Q_2]$, are given by:

$$Q_1 = \frac{\alpha}{a \cos\phi} \frac{\partial \mathbf{v}}{\partial \lambda} \cdot \nabla\theta$$
$$Q_2 = \frac{\alpha}{a} \frac{\partial \mathbf{v}}{\partial \phi} \cdot \nabla\theta \tag{5}$$

where $\alpha = -Rp^{R/c_p - 1}/p_0^{R/c_p}$, c_p is the specific heat, p_0 is the reference pressure and a is the radius of the earth.

Note that $\mathbf{Q} = \mathbf{Q}(\mathbf{v}, \theta)$ and, since $\mathbf{v}$ and θ both depend upon the stream function, that $\mathbf{Q}$ is a quadratic function of the stream function; this is of relevance in later sections. It is evident that (4) is frame-invariant and hence the attribution of vertical motion in terms of Q-vectors is unambiguous.

The use of this formulation of S for the attribution of vertical motion was described by Clough *et al.* (1996). Their approach was exploited by DBH who partitioned the $\nabla \cdot \mathbf{Q}$ distribution into upper- and lower-level slabs and applied the methodology to extratropical-cyclone classification. Whilst this procedure is valid, such a partitioning of the vertical motion is sometimes assumed to be either identical (or a close enough approximation) to a partitioning into upper- and lower-level slabs of PV. Here, we note that PV regions can lead to $\nabla \cdot \mathbf{Q}$ sources which (i) are located remotely from the PV, and (ii) are heavily dependent on other sources of PV. This is discussed more fully below; it suffices here to point out two implications of this in the context of layer-wise attribution. The first is that it is not possible to assess the contribution to the total vertical motion that is attributable to the upper-level PV distribution by simply calculating the vertical motion due to the upper-level $\nabla \cdot \mathbf{Q}$ distribution alone. Owing to the non-local nature of the $\mathbf{Q}$ field attributable to PV, the upper-level PV will lead to $\nabla \cdot \mathbf{Q}$ located in the lower atmosphere, and similarly low-level PV will lead to $\nabla \cdot \mathbf{Q}$ sources in the upper atmosphere. Secondly, the upper-level and lower-level PV sources, along with the non-local effects of the temperature at the boundaries, interact to form $\nabla \cdot \mathbf{Q}$ sources throughout both the upper and lower levels.

(*c*) *HMR formulation*

The formulation of the omega equation presented by HMR is illuminating as regards the physical origin of vertical motion, and proves to be useful in interpreting the new methodology presented in this paper.

The total vertical motion is given by:

$$\omega = \omega_{\mathrm{PVA}} + \omega_{\mathrm{IU}}. \tag{6}$$

Note that the contribution to the vertical motion due to the boundary temperature distribution is incorporated within ω_{PVA} by viewing that distribution as an infinitesimally thin sheet of PV located just above the surface (Bretherton 1966).

The PV advection (PVA) term is given by:

$$L(\omega_{\mathrm{PVA}}) = f_0 \frac{\partial}{\partial p}\{(\mathbf{v} - \mathbf{c}) \cdot \nabla_p q\} \tag{7}$$

where q is the PV and $\omega_{\mathrm{PVA}} = 0$ on the boundaries.

The isentropic up-glide term (IU), is evaluated *locally* and is given by:

$$\omega_{\mathrm{IU}} = -\frac{(\mathbf{v} - \mathbf{c}) \cdot \nabla_p \theta}{\mathrm{d}\theta_{\mathrm{ref}}/\mathrm{d}p} \tag{8}$$

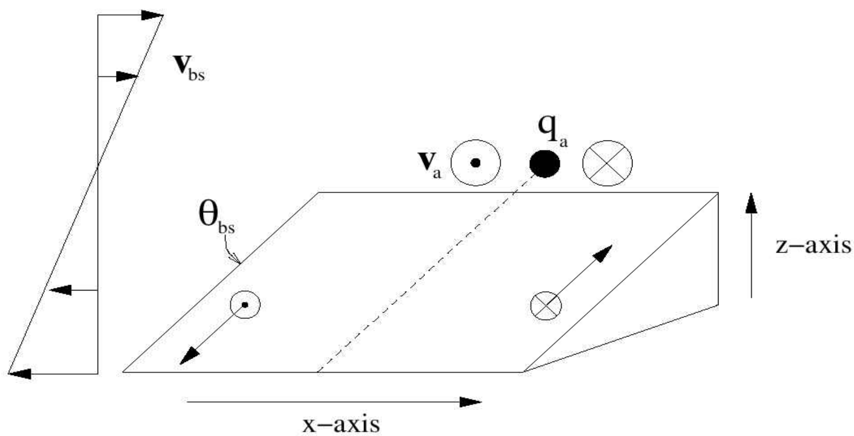

Figure 1. A schematic representation of how vertical motion arises from the interaction between (i) the horizontal wind fields (indicated by the circles) attributable to the point source of potential vorticity; and (ii) the sloping potential-temperature surfaces associated with the sheared flow of the basic state.

where θ_{ref} is the reference-state potential temperature.

Consider a system (Fig. 1) which consists of two separate regions of PV. The first region, q_{bs}, leads to an Eady-type basic state of constant shear, and the second region is a positive-valued point anomaly of PV, q_{a}, placed within that basic state. We assume that the basic state is constrained to be stationary, which implies the advection of q_{bs} by winds attributable to q_{a} has been neglected*.

In the rest frame of the anomaly, the total vertical motion is equal to ω_{IU}. We can therefore address the problem of attributing vertical motion by considering the isentropic-upglide velocity alone. Consider splitting the horizontal velocity, $\mathbf{v}$, and temperature, θ, into contributions attributable to q_{bs} and q_{a}, i.e. $\mathbf{v} = \mathbf{v}_{\mathrm{bs}} + \mathbf{v}_{\mathrm{a}}$ and $\theta = \theta_{\mathrm{bs}} + \theta_{\mathrm{a}}$. Substituting these decompositions into Eq. (8) leads to:

$$\begin{aligned}\omega_{\mathrm{IU}} \propto &- \mathbf{v}_{\mathrm{a}} \cdot \nabla_p \theta_{\mathrm{a}} - \mathbf{v}_{\mathrm{bs}} \cdot \nabla_p \theta_{\mathrm{bs}} \\ &- (\mathbf{v}_{\mathrm{a}} - \mathbf{c}) \cdot \nabla_p \theta_{\mathrm{bs}} - (\mathbf{v}_{\mathrm{bs}} - \mathbf{c}) \cdot \nabla_p \theta_{\mathrm{a}}. \end{aligned} \tag{9}$$

The two terms on the first line of (9) arise from fields attributable to one PV region alone. We refer to such contributions to the vertical motion as *self-generating*. In this case it is relatively straightforward to see that these terms are identically zero. However, if the anomaly, for example, were to be replaced with a non-symmetric distribution of PV, then its associated self-generated vertical motion would be finite. The resulting physical picture would also be complicated by the PVA term now being non-zero. We postpone consideration of such relatively more complicated cases until section 3.

The two terms on the second line of (9) are the *interaction* terms. The first of these corresponds to the horizontal velocity field attributable to the PV anomaly causing parcels to 'ride up' the tilted isentropes of the basic state (Fig. 1). The second (and smaller) term is due to the basic-state meridional velocity causing parcels to ride up the bent isentropes associated with the PV anomaly (Fig. 2).

This simple example serves to highlight the fact that vertical motion can arise from one PV region alone (the self-generating terms) or from two regions of PV

* This assumption may appear too restrictive and potentially pathological. Nevertheless, we use it here both because it is a commonly adopted procedure and is helpful in understanding the physical origin of vertical motion.

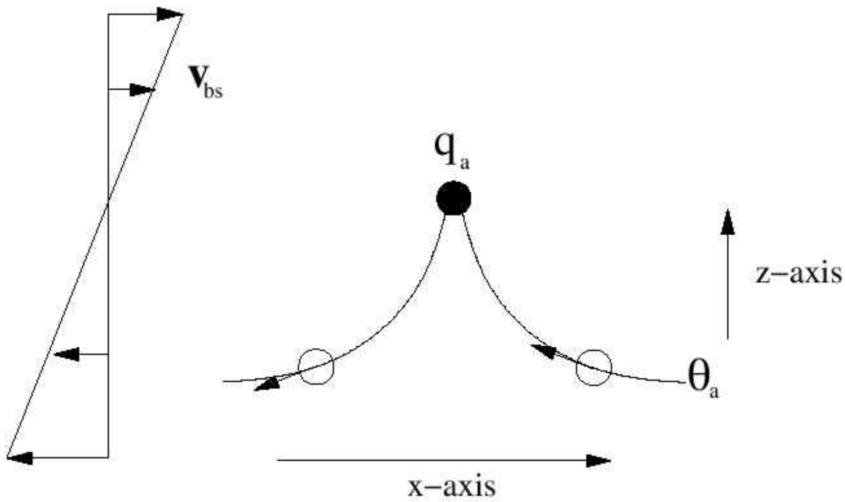

Figure 2. As Fig. 1, but here the vertical motion arises from the interaction between the basic-state wind and the potential-temperature field attributable to the PV anomaly.

(the interaction terms). We note that, whilst it is correct to talk of a particular self-generated component as being directly attributable to a given region of PV, it is misleading to claim that an interaction component is due to one PV region alone.

3. Layer-wise PV attribution of vertical motion

In this section it is shown how vertical motion may be explicitly attributed to layers of (interior and surface) PV. The process we adopt is essentially the same as that considered in the previous section, except that we adopt a Q-vector approach (which implicitly incorporates contributions from both the IU *and* the PVA terms). We first split the wind and potential-temperature fields, of which the source term (4) is a function, into parts that are attributable to each part of the PV distribution. These fields are, in turn, derived from the perturbation stream functions. The total perturbation stream function, ψ', can be obtained by inverting the QGPV equation:

$$\nabla_{\mathrm{h}}\psi' + \frac{\partial}{\partial p}\left(\frac{f_0}{\sigma}\frac{\partial\psi'}{\partial p}\right) = q \tag{10}$$

where ψ' is defined with respect to an averaged hydrostatic reference state and q is the total QGPV distribution within the region over which Eq. (10) is to be inverted. We could partition this interior PV into as many components as we wish. However, investigations of attribution (including that of DBH) are often posed in terms of the relative importance of the upper and lower levels of the atmosphere. For this reason we have chosen to partition q into upper- and lower-level slabs, leading to associated stream functions defined as follows:

1. ψ'_{U}—the stream function that is attributable to all of the PV located in the 'upper levels', q_{U} (defined to be the layer ranging from 600 mb to 150 mb, inclusively),
2. ψ'_{L}—the stream function that is attributable to all of the PV located in the 'lower-levels', q_{L} (i.e. 950 mb to 650 mb, inclusive),

where we have assumed that the PV and all other fields are defined on a grid of 50 mb vertical resolution.

The layer-wise inversion process involves an arbitrary choice of boundary conditions. The procedure usually adopted is to set the vertical derivative of the stream function (or, equivalently, the potential temperature) equal to zero on the horizontal boundaries, so that the temperature on the boundaries may be considered as a separate distribution whose evolution is coupled to that of the interior PV via horizontal winds alone. In what follows, we set the temperature at the lower and upper surfaces (i.e. 1000 mb and 100 mb) attributable to the interior PV (be it 'upper' or 'lower') to zero. On the other boundaries, $\psi'_{\mathrm{U}} = \psi'_{\mathrm{L}} = 0$.

It follows that there is a third contribution to the total perturbation stream function, which we shall refer to as the boundary component:

$$\psi'_{\mathrm{B}} = \psi' - (\psi'_{\mathrm{U}} + \psi'_{\mathrm{L}}). \tag{11}$$

This boundary component can be further divided into two sub-components*. The first part is due to the temperature distributions on the upper and lower boundaries, which (as mentioned above) can be viewed as infinitesimally-thin sheets of PV. The second component arises from the lateral boundary conditions. We assume that, as long as the stream function is evaluated close to the lower boundary and far from the lateral boundaries, ψ'_{B} (and, indeed, any vertical motion that is attributable to it) will be dominated by the effects of the lower-boundary temperature (or PV sheet) distribution. This approximation is valid at each position of the cyclones considered in the next section. In summary, we have effectively partitioned the total PV distribution into three parts: two interior slabs and a lower-boundary sheet. We now wish to determine the vertical motion attributable to these regions.

Now, because of (1) and as $\mathbf{Q} = \mathbf{Q}(\mathbf{v}, \theta)$, we can write symbolically that $\omega = \omega(\mathbf{v}, \theta)$. As $\mathbf{Q}$ depends on the products of $\mathbf{v}$ and θ then, if we partition $\mathbf{v}$ and θ into three components each, the result is that there are nine individual terms for ω. Therefore, if the wind and potential-temperature fields in (4), which are related to the horizontal and vertical derivatives of the stream function, are partitioned into the three components corresponding to the stream functions defined above, then (2) leads to the following key expression for the total vertical motion:

$$\begin{aligned}\omega = {} & \omega(\mathbf{v}_{\mathrm{U}}, \theta_{\mathrm{U}}) + \omega(\mathbf{v}_{\mathrm{L}}, \theta_{\mathrm{L}}) + \omega(\mathbf{v}_{\mathrm{B}}, \theta_{\mathrm{B}}) \\ & + \omega(\mathbf{v}_{\mathrm{U}}, \theta_{\mathrm{L}}) + \omega(\mathbf{v}_{\mathrm{L}}, \theta_{\mathrm{U}}) \\ & + \omega(\mathbf{v}_{\mathrm{U}}, \theta_{\mathrm{B}}) + \omega(\mathbf{v}_{\mathrm{B}}, \theta_{\mathrm{U}}) \\ & + \omega(\mathbf{v}_{\mathrm{L}}, \theta_{\mathrm{B}}) + \omega(\mathbf{v}_{\mathrm{B}}, \theta_{\mathrm{L}}).\end{aligned} \tag{12}$$

The three velocities on the first line of (12) represent the self-generating terms which, as in section 2(c), are each due to the interaction of the potential-temperature and wind fields attributable to one element alone. Thus, for example, the first term corresponds to the vertical motion associated with the upper-level PV distribution alone. The final three lines of (12) contain the interaction terms which arise from the temperature field attributable to one layer interacting with the winds of another layer and vice versa†.

* Note that a component of ψ'_{B} corresponding to a particular boundary could be determined via an inversion of Eq. (10), with the interior PV set to zero and the conditions stated earlier (i.e. either the stream function or potential temperature set to zero) imposed at the other boundaries.

† Note that, if we partitioned the stream function in the way described and then calculated the resulting *sum* of the PVA and IU terms or the *sum* of the TA and VA terms due to each of the nine combinations of temperature and velocity fields, then we would necessarily arrive at the same decomposition stated in (12).

Since both the potential-temperature and horizontal-velocity fields are derived from stream functions, arguably it would be more meaningful to decompose the vertical motion in terms of the stream functions alone. This would lead to a total of six components, as opposed to the nine in (12). If we write

$$\begin{aligned} \omega(\mathbf{v}_\mathrm{U}, \theta_\mathrm{U}) &= \omega(\mathrm{U}, \mathrm{U}) \\ \omega(\mathbf{v}_\mathrm{L}, \theta_\mathrm{L}) &= \omega(\mathrm{L}, \mathrm{L}) \\ \omega(\mathbf{v}_\mathrm{B}, \theta_\mathrm{B}) &= \omega(\mathrm{B}, \mathrm{B}) \end{aligned} \tag{13}$$

and also,

$$\begin{aligned} \omega(\mathbf{v}_\mathrm{L}, \theta_\mathrm{U}) + \omega(\mathbf{v}_\mathrm{U}, \theta_\mathrm{L}) &= \omega(\mathrm{U}, \mathrm{L}) \\ \omega(\mathbf{v}_\mathrm{U}, \theta_\mathrm{B}) + \omega(\mathbf{v}_\mathrm{B}, \theta_\mathrm{U}) &= \omega(\mathrm{U}, \mathrm{B}) \\ \omega(\mathbf{v}_\mathrm{L}, \theta_\mathrm{B}) + \omega(\mathbf{v}_\mathrm{B}, \theta_\mathrm{L}) &= \omega(\mathrm{L}, \mathrm{B}) \end{aligned} \tag{14}$$

then we can write the sum of the six terms as:

$$\begin{aligned} \omega = {} & \omega(\mathrm{U}, \mathrm{U}) + \omega(\mathrm{L}, \mathrm{L}) + \omega(\mathrm{B}, \mathrm{B}) \\ & + \omega(\mathrm{U}, \mathrm{L}) + \omega(\mathrm{U}, \mathrm{B}) + \omega(\mathrm{L}, \mathrm{B}). \end{aligned} \tag{15}$$

In section 4 we consider the decomposition given by (15); however, we also make use of the decomposition given by (12), both for the sake of completeness and because this decomposition provides a more direct physical understanding (analogous to the example given in section 2(c) above).

The approach adopted by studies such as those of Davis (1992) and Griffiths *et al.* (2000), adapted to the present context, can be understood as follows. The vertical motion attributable to, for example, the upper-level PV slab would be given by:

$$\omega_\mathrm{U} = \omega(q) - \omega(q - q_\mathrm{U}). \tag{16}$$

This expression can be straightforwardly rewritten by substituting in the terms of Eq. (15):

$$\omega_\mathrm{U} = \omega(\mathrm{U}, \mathrm{U}) + \omega(\mathrm{U}, \mathrm{L}) + \omega(\mathrm{U}, \mathrm{B}). \tag{17}$$

An expression for the vertical motion nominally attributable to the lower-level PV can be similarly obtained:

$$\omega_\mathrm{L} = \omega(\mathrm{L}, \mathrm{L}) + \omega(\mathrm{U}, \mathrm{L}) + \omega(\mathrm{L}, \mathrm{B}). \tag{18}$$

As ω_U and ω_L both contain the component $\omega(\mathrm{U}, \mathrm{L})$, this form of attribution is non-unique. By way of contrast, our methodology explicitly identifies the interaction terms such as $\omega(\mathrm{U}, \mathrm{L})$.

In the context of QGPV, the method of attribution adopted by Morgan (1999) amounts to partitioning $\mathbf{Q}$ in terms of horizontal velocity *only* and treating the potential temperature field as a given quantity (i.e. effectively independent of the PV), leading to $\omega = \omega(\mathbf{v}_\mathrm{U}, \theta) + \omega(\mathbf{v}_\mathrm{L}, \theta) + \omega(\mathbf{v}_\mathrm{B}, \theta)$. Since this expression does not include interaction terms there is no uniqueness problem*. By way of contrast, our methodology also allows for the attribution of potential temperature to the PV distribution.

4. Application: Attribution of cyclone forcing

In this section, we apply the layer-wise attribution of vertical motion to determine the role PV layers play in the development of extratropical cyclones.

* In the paper by Morgan (1999) the QG vertical motion is attributed to regions of an approximate form of Ertel–Rossby PV. In that case, non-uniqueness arises because of the nonlinearity of the equation for PV.

(*a*) *Method*

In what follows, we interpret the rate of 'development' as the rate of change in vorticity following a cyclone. We define the cyclone location as the position of the local minimum of geopotential on the 900 mb level. The material derivative D_t^c of geostrophic vorticity, ξ, evaluated using the velocity, $\mathbf{c}$, of the cyclone centre is given by:

$$D_t^c(f+\xi) = (\mathbf{c}-\mathbf{v}) \cdot \nabla(f+\xi) + f\frac{\partial\omega}{\partial p}. \tag{19}$$

The advection term can be assumed to be small in the cyclone's frame of reference, and hence (19) may be approximated as:

$$D_t^c(f+\xi)|_{900\,\mathrm{mb}} \approx \frac{f}{\Delta}(\omega|_{800\,\mathrm{mb}} - \omega|_{\mathrm{surface}}) = \frac{f}{\Delta}\omega|_{800\,\mathrm{mb}} \tag{20}$$

where the omega at 1000 mb has been set to zero and Δ is equal to 200 mb. We make the assumption that the overall forcing of the cyclone can be assessed by measuring the forcing at the position of maximum development. We identify this position as the grid point corresponding to the local maximum vertical motion on the 800 mb surface. Attributing the cyclone development to layers of PV amounts to evaluating (20) at this point using each of the components given in (12) or (15). Henceforth, when we refer to any of the component terms of these two equations we will be implicitly referring to their values at this point. We have applied the methodology described to a number of cyclones but, before presenting the results, we first discuss the physical interpretation of the methodology in more detail and highlight some features which we expect to be shared by *all* cyclones.

(*b*) *Physical interpretation*

(i) *The PV distribution in a midlatitude cyclone.* Figure 3 shows a schematic cross-section through a midlatitude cyclone. The upper-level PV distribution may be viewed as consisting of two components: the large-scale PV transition associated with the sloping tropopause, and a smaller-scale PV 'anomaly' identified as a local 'fold' in the tropopause. In the lower levels, the background PV is small and homogeneous, with local PV anomalies (ultimately due to diabatic and frictional effects) dominating. Also evident in Fig. 3 is the lower-boundary potential-temperature distribution. It is important to note a distinction between the case depicted in Fig. 3 and that of the idealized example of section 2(c). In the idealized case, the basic-state wind and potential-temperature fields are attributable to a PV distribution that is (artificially) unaffected by the PV within the system. In contrast, the large-scale fields in Fig. 3 are attributable to both the interior PV and the boundary conditions. In fact, they are mainly a consequence of the PV associated with the sloping tropopause and the surface temperature gradient, with the anomalies making a smaller contribution.

(ii) *The self-generating terms.* Consider the self-generating terms of (12). Imagine a PV anomaly placed within a barotropic basic state. If the anomaly is symmetrical (in the QG-scaled coordinate $\sqrt{x^2+y^2+\sigma^2p^2/f_0^2}$) then it is straightforward to show that no vertical motion will be generated. Thus, for example, the point PV anomaly considered in section 2(c) has no self-generated vertical motion associated with it. The same would be true of the low-level PV region in Fig. 3 if the low-level anomaly were perfectly symmetrical. As this is not true in general, $\omega(\mathrm{L}, \mathrm{L})$ will be finite and, hence, contribute to the cyclone's development.

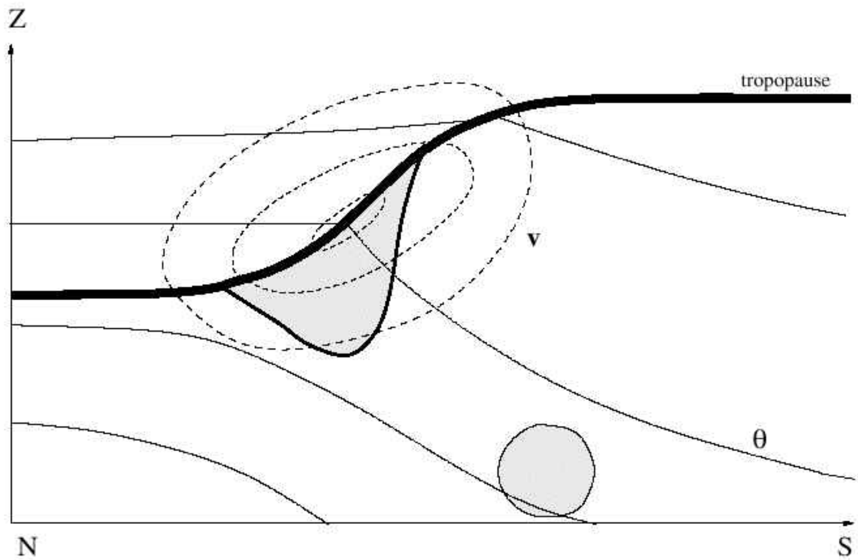

Figure 3. A schematic cross-section through a midlatitude cyclone. A few contours of horizontal wind (dashed lines) and potential temperature (full lines) are shown. The tropopause marks the large-scale potential-vorticity (PV) transition (thick line). An upper-level PV anomaly, or tropopause fold, (dashed lines) and a lower-level anomaly (circular contour) are also shown.

The nature of the upper-level PV self-generated motion, $\omega(\mathrm{U}, \mathrm{U})$, is complicated by the presence of the PV associated with the sloping tropopause. Part of $\omega(\mathrm{U}, \mathrm{U})$ will be due to the interaction between the fields attributable to the large-scale PV transition and those fields attributable to the local PV anomaly. In addition, if the PV anomaly displays asymmetry, then part of $\omega(\mathrm{U}, \mathrm{U})$ will be due to the anomaly alone. If there are no upper-level PV anomalies, on the other hand, then $\omega(\mathrm{U}, \mathrm{U})$ will be zero.

The self-generating contribution to cyclone development from the lower-boundary term, $\omega(\mathrm{B}, \mathrm{B})$, is likely to be small. This can be understood by interpreting our methodology in terms of the Eady problem (see, for example, Davies and Bishop (1994)). In that problem, edge waves constrained to the upper and lower boundaries grow in amplitude owing to their interaction. This interaction is mediated via the basic state of uniform baroclinic shear. Note that, just as in section 2(c), the basic state of the Eady problem is artificially decoupled from the dynamical evolution of the system. Nevertheless, the PV distribution on the lower boundary may be thought of as an edge wave and, as such, the wind and potential temperature fields attributable to this distribution will act in such a way as to propagate the surface temperature anomaly without any concomitant growth. Analogous to an edge wave, this distribution will have no associated self-generated vertical motion; it is only via the interaction with the basic state that growth and vertical motion occur.

(iii) *Interaction terms.* For any of the interaction terms to be finite, the morphology of the two relevant regions of PV must differ. To see this, imagine a symmetrical anomaly, such as the point anomaly of section 2(c), in a barotropic background flow. The introduction of a second anomaly, identical in shape at the same position as the first, would not lead to any vertical motion. It is only by shifting the relative positions of the anomalies and/or altering their shapes, that any 'interaction' vertical motion can be generated. One would expect there to be much scope for differences between the morphologies of the three PV regions in a midlatitude cyclone, implying that the interaction terms may play an important role in cyclone development.

Of all the interaction terms, it is likely that $\omega(\mathrm{L}, \mathrm{B})$ will play the most significant role in most cyclones. This is simply because of the relative proximity of a low-level PV anomaly and of the boundary PV distribution to the location of the cyclone. The wind and potential temperature fields attributable to both of these PV regions will be large in the vicinity of the cyclone and, as long as these fields differ significantly in terms of their morphology, they will lead to large $\nabla \cdot \mathbf{Q}$ and hence large vertical motion close to the cyclone. Owing to the greater distance between the upper-level PV and the cyclone, we may expect $\omega(\mathrm{U}, \mathrm{B})$ and $\omega(\mathrm{U}, \mathrm{L})$ to be less significant than $\omega(\mathrm{L}, \mathrm{B})$, in general.

Of the two components of $\omega(\mathrm{L}, \mathrm{B})$, it is likely that $\omega(\mathbf{v}_\mathrm{L}, \theta_\mathrm{B})$ will be larger than $\omega(\mathbf{v}_\mathrm{B}, \theta_\mathrm{L})$. This difference can be understood by referring to the idealized example presented in section 2(c). Since the sign of θ_a changes with height, the $\nabla \cdot \mathbf{Q}$ distribution that is attributable to θ_a and $\mathbf{v}_\mathrm{bs}$ forms a vertical dipole. The resulting vertical motion is relatively smaller than that associated with θ_bs and $\mathbf{v}_\mathrm{a}$, owing to destructive interference between the two parts of the aforementioned dipole. We can apply such reasoning to the real case of $\omega(\mathrm{L}, \mathrm{B})$, since the low-level PV tends to be relatively localized and the fields associated with the boundary PV are similar to that of the basic state in the idealized example. However, the reasoning may be less relevant in the case of $\omega(\mathrm{U}, \mathrm{B})$ and its component elements because, although the upper-level PV distribution may contain anomalies, it is also composed of the transition associated with the sloping tropopause (which bears a strong resemblance to the boundary PV distribution).

(*c*) *FASTEX case studies*

The methodology described above has been applied to a total of four cyclones which occurred during the Fronts and Atlantic Storm-Tracks Experiment (FASTEX) campaign (see Joly *et al.* 1999). So as to highlight the differences between our new approach and that of the method by which cyclone forcing is attributed to parts of the $\nabla \cdot \mathbf{Q}$ distribution, these cyclones have been picked according to the classification scheme of DBH, which assessed the forcing of each cyclone in terms of the vertical motion at 700 mb*. In addition to the Type A and B cyclones proposed in the original PS scheme, DBH identified Type C cyclones, which are more strongly upper-level forced than those of Type B. The four cyclones considered below, labelled by their FASTEX 'Intensive Observation Period' (IOP) numbers, were chosen according to the following criteria. IOP9 and IOP14 were the strongest low-level forced Type A cyclones; IOP11A was a middle-of-the-range Type B cyclone; and IOP18 was the strongest upper-level forced Type C cyclone.

The data used are analyses and T+3 forecasts from the operational Met Office limited area model. The total perturbation stream function, ψ', is used to derive the interior QGPV on 50 mb levels ranging from 950 mb to 150 mb. The essential features that determined each cyclone's type (according to the DBH scheme) occurred during the sampling periods of this investigation. The average distance (during the sampling period of all the cyclones) between the boundaries and the point at which Eq. (20) was evaluated was $\approx$3000 km. The minimum value obtained of this separation distance was $\approx$1000 km.

* There are a number of differences, including the choice of level on which the vertical motion is calculated, between our approach and that of DBH. However, we are using the results of DBH as a guide to the type of cyclones studied, and these differences have little effect on the conclusions drawn here.

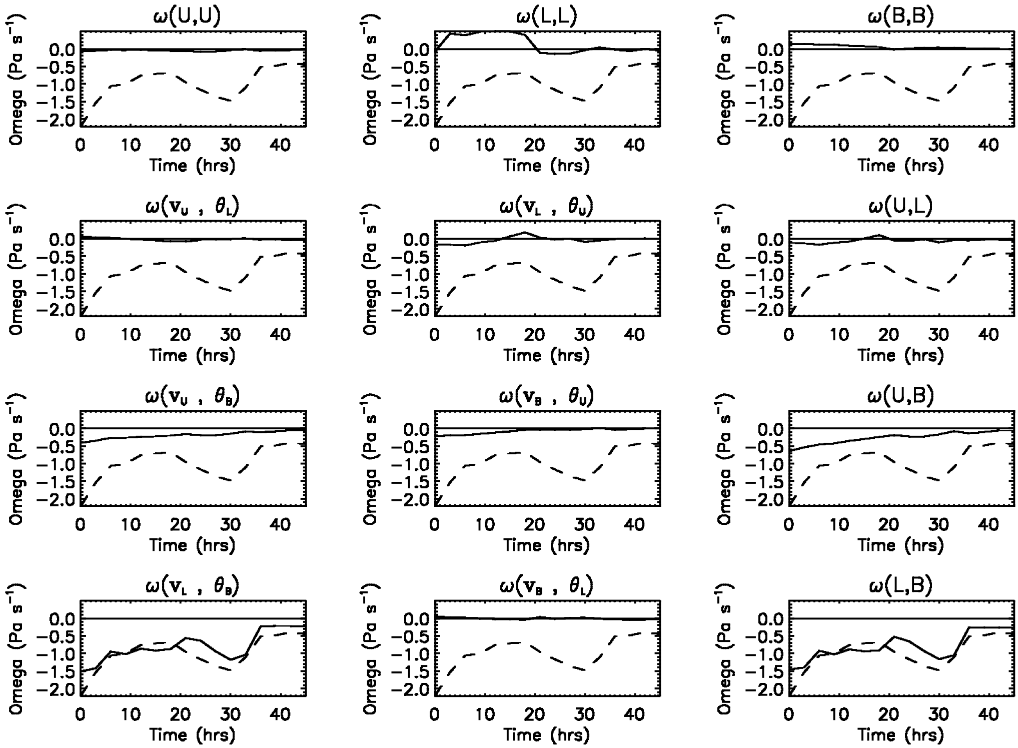

Figure 4. The time-series of the vertical velocity (Omega) (dashed lines) and its constituent parts (full lines) at the position of maximum ascent in the case of the cyclone of IOP14. The top row of three plots are the self-generating terms. The remaining three rows of plots are the interaction terms. The first two plots in each row represent the potential-temperature and horizontal-wind decompositions of the vertical velocity, and the third plot in the row shows the sum of these two terms, i.e. the decomposition in terms of stream function alone.

(i) *Resulting characteristics of FASTEX cyclones.* An inspection of Figs. 4–7 reveals that the most striking overall differences in forcing are between, on the one hand, the Type A and B cyclones (i.e. IOP9, 14 and 11A) and, on the other hand, the Type C cyclone, IOP18. This latter cyclone had the deepest tropopause fold of any throughout the FASTEX period; hence, it might be expected that the upper-level PV distribution played a large role in the forcing of this cyclone. The time series shown in Fig. 7 corresponds to a period of significant cyclonic deepening, during which a large upper-level PV anomaly appears to interact with the cyclone. As can be seen in Fig. 7, one of the main individual contributions to the forcing is that of the upper-level PV self-generating term, $\omega(\mathrm{U}, \mathrm{U})$. There are two interrelated reasons for this: (a) the upper-level PV anomaly is large enough in IOP18 to produce a significant $\nabla \cdot \mathbf{Q}$ field via the interaction with the remaining part of the upper-level PV distribution which is attributable to the sloping tropopause; and (b) the upper-level anomaly in IOP18 is located relatively far down into the troposphere, so the associated $\nabla \cdot \mathbf{Q}$ is large in the region close to the cyclone.

In the other cyclones $\omega(\mathrm{U}, \mathrm{U})$ is relatively small, attaining its largest values in the Type B, IOP11A. In the Type A and B cyclones, the upper-level PV distribution tends to be relatively 'anomaly-free', dominated instead by the sloping tropopause (in contrast to point (a) mentioned above). Hence, the vertical motion related to the upper-level PV in the Type A and B cyclones is mainly due to the interaction of the essentially zonally

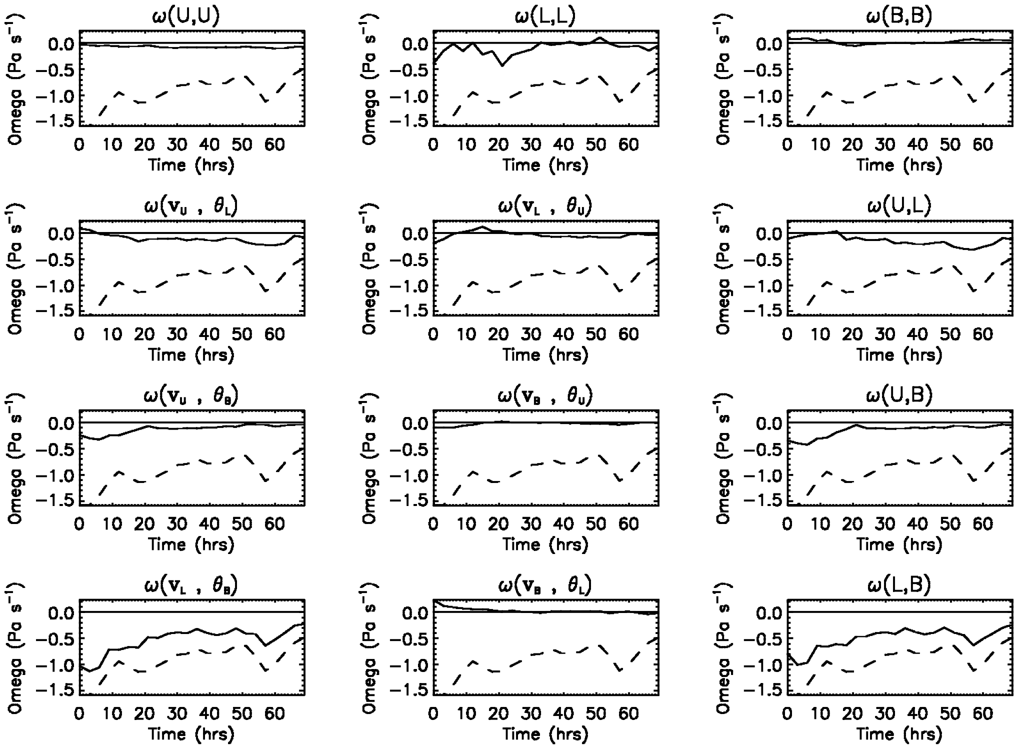

Figure 5. As Fig. 4, but for the case of IOP9.

aligned stream function (which results from the meridional PV gradient) with the stream functions attributable to the more inhomogeneous low-level PV and/or surface temperature distribution. Moreover, these contributions are larger than any upper-level self-generated vertical motion which *does* exist, owing to the relative closeness of the low-level and boundary PV distributions to the cyclone.

The other important individual forcing term in IOP18 is $\omega(\mathbf{v}_\mathrm{L}, \theta_\mathrm{B})$. As was proposed in the previous section, this term should be large in *all* of the cyclones studied. It is worth stressing that this is the case even for a cyclone such as IOP18 where the upper-level PV anomaly is strikingly large. In other words, from a PV perspective, it appears that the low levels are always important. Note that the terms $\omega(\mathrm{L}, \mathrm{L})$, $\omega(\mathrm{U}, \mathrm{L})$ and $\omega(\mathrm{U}, \mathrm{B})$ are also important in IOP18. While each term on its own is (for most of the period) of secondary importance, their combined effect is, nevertheless, significant.

In the Type A cyclones (Figs. 4 and 5), the single most dominant component is $\omega(\mathbf{v}_\mathrm{L}, \theta_\mathrm{B})$. However, in a similar fashion to IOP18, $\omega(\mathrm{L}, \mathrm{L})$, $\omega(\mathrm{U}, \mathrm{L})$ and $\omega(\mathrm{U}, \mathrm{B})$ all contribute significantly. Note that, while at first sight $\omega(\mathbf{v}_\mathrm{L}, \theta_\mathrm{B})$ in IOP14 might appear to be the only term of importance, there is large cancellation between terms ($\omega(\mathrm{L}, \mathrm{L})$ is positive), and both $\omega(\mathrm{L}, \mathrm{L})$ and $\omega(\mathrm{U}, \mathrm{B})$ also attain relatively large magnitudes. In the Type B cyclone, IOP11A (Fig. 6), it appears that the tropopause fold is strong enough so that the self-generating term $\omega(\mathrm{U}, \mathrm{U})$ is slightly larger than in the Type A cyclones. However, this term is much smaller than in the case of IOP18, and the main involvement of the upper-level PV is still via the interaction terms. Note that, in the Type B cyclone, the upper-level PV plays a larger role early on and $\omega(\mathbf{v}_\mathrm{L}, \theta_\mathrm{B})$ becomes more significant at later stages. Such behaviour is less clear in the case of the Type A cyclones, and it is

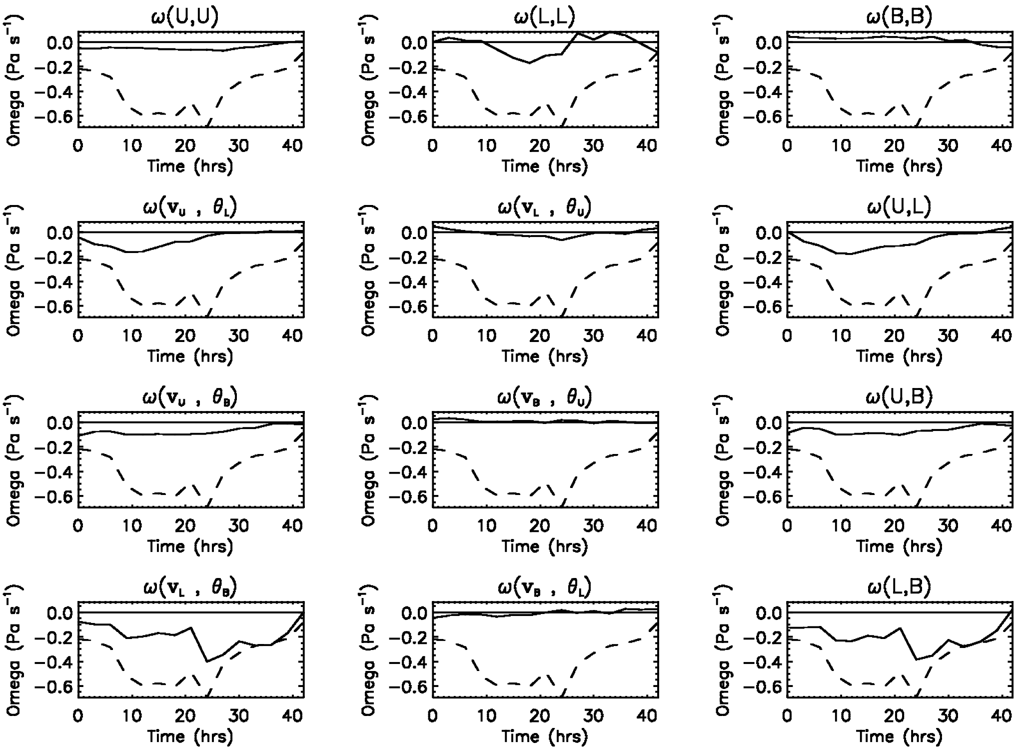

Figure 6. As Fig. 4, but for the case of IOP11A.

tempting to speculate that the upper-level PV anomaly in the Type B cyclone in some sense causally precedes the lower-level PV. (The period over which the Type B cyclone is sampled begins when the DBH method shows a large upper-level contribution.)

From a PV perspective, the differences between the Type A and Type B cyclones appear to be more differences of degree than of kind. Whether or not we choose to view these relatively subtle differences as constituting different *classes* of cyclone from a 'PV-thinking' viewpoint is a matter of debate that could be addressed by investigating many more cyclones. However, it is clear that the role played by the upper-level PV differs markedly between the Type C cyclone (during the period sampled) and the other cyclones. Hence, from a PV-attribution viewpoint of instantaneous cyclone forcing, there appear to be two main classes of cyclone: one where the effect of the upper-level PV is predominantly due to the interaction with the low-level PV and/or surface PV; and another where the self-generating vertical motion of the upper-level PV plays a large role during part of the cyclone's lifetime.

(*d*) *Time-integrated effects and PV-surgery*

The methodology presented here does not address to what extent one region of PV influences the development of either itself or another region of PV and/or the boundary component. Such *time-integrated* effects are important in that they lead to a more complete causal description of the cyclone's evolution, which cannot be inferred by considering alone the *instantaneous* role of a PV region (as assessed via Eq. (20)). For example, in the case of IOP18 we have shown that, even though the upper-level PV

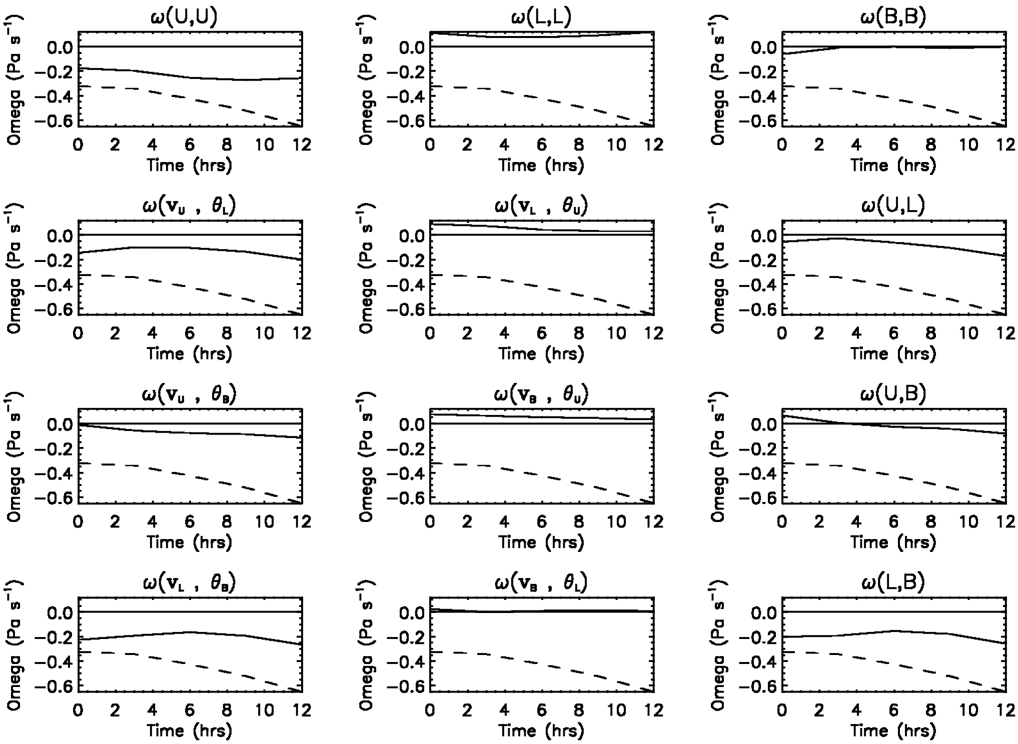

Figure 7. As Fig. 4, but for the case of IOP18.

contributes a large amount to the development of the cyclone, the $\omega(\mathbf{v}_L, \theta_B)$ is just as significant in the same instantaneous sense. However, this does not imply that the low-level PV is necessarily as important as the upper-level PV in determining the overall evolution of the cyclone. As the upper-level PV produces, by itself, a significant amount of vertical motion in the low-levels, it is likely that it is responsible for a significant amount of the diabatic production of PV in that region. Furthermore, the advection of the low-level PV is probably dominated by the horizontal winds attributable to the upper-level PV. If it also transpires that the low-level PV has very little effect on the upper-level PV, then the cyclone might be said to be ultimately forced by the upper-level PV. By way of contrast in the case of IOP14, where the upper-level PV is less significant, it may be that low-level PV is responsible for its own development so that the cyclone is forced largely by the low-level PV and boundary components.

The distinction between instantaneous and time-integrated forcing is related to the difference between the form of instantaneous attribution described and adopted in this paper and the related methodology of so-called prognostic PV-surgery. In the latter method, the impact on dynamical development attributable to a particular region of PV is assessed by taking the difference between a model run where the fields attributable to the region are removed and a control run where the fields are unaltered. Such a procedure directly yields information on the effect of the region on development. However, it suffers from two drawbacks: (i) it fails to make the distinction between self-generating and interaction forcing; and (ii) the system is changed by the removal of PV, whereas the methodology presented here assesses the role of PV in the unaltered system. On the other hand, prognostic PV-surgery avoids having to assess explicitly both the instantaneous and time-integrated importance of PV and can easily incorporate the effects of diabatic processes. Notwithstanding these differences, we might expect the two methodologies to yield similar results. According to the prognostic PV-surgery described by Ahmadi-Givi and Craig (personal communication), the development of the Type C cyclone of IOP18 is dramatically diminished when the upper-level PV anomaly is removed and the upper-level PV anomaly fails to fully redevelop. On the other hand, their experiments where the low-level PV anomaly was removed led to less of an impact on development and the low-level PV was seen to redevelop. Furthermore, by considering the instantaneous fields attributable to each of the PV regions, they established that the evolution of the upper-level PV was essentially controlled by upper-level dynamics. Hence, both prognostic PV-surgery and the methodology of the present study (when time-integrated forcing is taken into account) suggest that, in the case of the Type C cyclone, the upper-level PV dominates the development of the cyclone.

5. Conclusions

The methodology presented in this paper enables the vertical motion attributable to a region of PV to be determined in an explicit manner, thereby providing a direct link between PV and dynamical development. It has been shown how the total vertical motion may be decomposed into a number of self-generating and interaction terms that are uniquely related to regions of PV. The self-generating terms correspond to the vertical motion that arises from one region of PV, whilst each interaction term results from the combined effect of two different regions of PV. The existence of the interaction terms, which makes the PV attribution of vertical motion more complicated than the more traditional forms of vertical-motion attribution, is a consequence of the quadratic dependence of the vertical motion on stream function. It is possible to regard the interaction terms as arising from either the stream functions attributable to each of the two regions of PV, or from the horizontal velocity attributable to one PV region and the potential temperature attributable to the other region.

Vertical motion is a key quantity in diagnosing dynamical development, and we have used the new methodology to assess the development of five FASTEX cyclones. We chose to partition the total PV distribution into three layers (upper, lower and lower boundary) for the purposes of simplicity and to facilitate comparison with the extended Petterssen–Smebye scheme of DBH. The method could, however, be applied using any other desired decomposition.

Each cyclone exhibited a number of common features, which we have been able to explain in terms of general principles. Of central importance in all of the cases studied, is the dominance of the term that arises from the interaction between the horizontal velocity attributable to the lower-level layer of PV and the potential temperature attributable to the boundary PV. This is due to the proximity of both PV regions to the cyclone location.

DBH classified cyclones into Types A, B and C. Types A and B correspond to the earlier classification of Petterssen and Smebye (1971) and Type C is an additional category strongly forced from upper levels. From a PV perspective, we found that there were only subtle differences between the Type A and B cyclones. For example, the upper-level PV layer played a more important role in the case of the Type B case. We have found that the most striking difference exhibited was between the Type A and B cyclones on the one hand, and the Type C cyclone on the other. A large enough upper-level PV anomaly was present during part of the Type C cyclone's lifetime for the self-generating term associated with the upper-level PV to play a significant role in the forcing. In the Type A and B cyclones, however, the upper-level anomalies were not strong enough to have a major effect in themselves and the main influence of the upper-level PV was via interaction with the two lower PV regions.

It is worth stressing that, even in the case of the Type C cyclone, the low-level forcing term described above still played a very significant role. Hence, from the viewpoint of instantaneous forcing, the low-level PV is important even when there is a very strong upper-level PV anomaly present. However, in the case of the Type C cyclone, we have also argued, from the viewpoint of time-integrated forcing, that the upper-level PV is likely to be of greatest importance since it appears to generate and/or control low-level PV via its self-generating term.

The extent to which these case studies are representative of cyclones in general can only be gauged by applying the new methodology to a much larger sample of cyclones. Such a procedure would be relatively straightforward to implement in an automated fashion.

Acknowledgements

We are grateful for the European Union's FASTEX-CSS contract (ENV4-CT97-0625) which funded this work. We also thank Drs Paul Berrisford, Ross Bannister and Sid Clough for useful discussions and we are grateful for the comments of two anonymous referees.

References

Bishop, C. H. and Thorpe, A. J. 1994 Potential vorticity and the electrostatic analogy: Quasi-geostrophic theory. *Q. J. R. Meteorol. Soc.*, **120,** 713–731

Bretherton, F. P. 1966 Critical layer instability in baroclinic flows. *Q. J. R. Meteorol. Soc.*, **92,** 325–334

Clough, S. A., Davitt, C. S. A. and Thorpe, A. J. 1996 Attribution concepts applied to the omega equation. *Q. J. R. Meteorol. Soc.*, **122,** 1943–1962

Davies, H. C. and Bishop, C. H. 1994 Eady edge waves and rapid development. *J. Atmos. Sci.*, **51,** 1930–1946

Davis, C. A. 1992 A potential vorticity diagnosis of the importance of initial structure and condensational heating on observed extra-tropical cyclogenesis. *Mon. Weather Rev.*, **120,** 2409–2428

Davis, C. A. and Emanuel, K. A. 1991 Potential vorticity diagnostics of cyclogenesis. *Mon. Weather Rev.*, **119,** 1929–1953

Deveson, A. C., Browning, K. A. and Hewson, T. D. 2002 A classification of FASTEX cyclones using a height-attributable quasi-geostrophic vertical-motion diagnostic. *Q. J. R. Meteorol. Soc.*, **128,** 93–117

Griffiths, M., Thorpe, A. J. and Browning, K. A. 2000 Convective destabilization by a tropopause fold diagnosed using potential-vorticity inversion *Q. J. R. Meteorol. Soc.*, **126,** 125–144

Hoskins, B. J., Draghici, I. and Davies, H. C. 1978 A new look at the ω equation. *Q. J. R. Meteorol. Soc.*, **104,** 31–38

Hoskins, B. J., McIntyre, M. E. and Robertson, A. W. 1985 On the use and significance of isentropic potential vorticity maps. *Q. J. R. Meteorol. Soc.*, **111,** 877–946

Joly, A., Browning, K. A., Bessemoulin, P., Cammas, J. P., Caniaux, G., Chalon, J. P., Clough, S. A., Dirks, R., Emanuel, K. A., Eymard, L., Gall, R., Hewson, T., Hildebrand, P. H., Jorgensen, D., , Lalaurette, F., Langland, R. H., Lemaitre, Y., Mascart, P., Moore, J. A., Roux, P. F., Persson, P. O. G., Shapiro, M. A., Snyder, C. and Toth, Z. 1999 Overview of the field phase of the Fronts and Atlantic Storm-Track Experiment (FASTEX) project. *Q. J. R. Meteorol. Soc.*, **125,** 3131–3165

Morgan, M. C. 1999 Using piecewise potential vorticity inversion to diagnose frontogenesis. Part I: A partitioning of the Q vector applied to diagnosing surface frontogenesis and vertical motion. *Mon. Weather Rev.*, **127,** 2796–2821

Petterssen, S. and Smebye, S. J. 1971 On the development of extratropical cyclones. *Q. J. R. Meteorol. Soc.*, **97,** 457–482

Stoelinga, M. T. 1996 A potential vorticity based study of the role of diabatic heating and friction in a numerically simulated baroclinic cyclone. *Mon. Weather Rev.* , **124,** 849–874

Swarbrick, S. 2001 Applying the relationship between potential vorticity fields and water vapour imagery to adjust initial conditions in NWP. *Meteorol. Appl.*, **8,** 221–228

Thorpe, A. J. 1997 Attribution and its application to mesoscale structure associated with tropopause folds. *Q. J. R. Meteorol. Soc.*, **123,** 2377–2400